Antibody Modification

International Edition: DOI: 10.1002/anie.201411507
German Edition: DOI: 10.1002/ange.201411507

A Versatile Approach for the Site-Specific Modification of Recombinant Antibodies Using a Combination of Enzyme-Mediated Bioconjugation and Click Chemistry**

Karen Alt, Brett M. Paterson, Erik Westein, Stacey E. Rudd, Stan S. Poniger, Shweta Jagdale, Katie Ardipradja, Timothy U. Connell, Guy Y. Krippner, Ashish K. N. Nair, Xiaowei Wang, Henri J. Tochon-Danguy, Paul S. Donnelly,* Karlheinz Peter, and Christoph E. Hagemeyer**

Abstract: *A unique two-step modular system for site-specific antibody modification and conjugation is reported. The first step of this approach uses enzymatic bioconjugation with the transpeptidase Sortase A for incorporation of strained cyclooctyne functional groups. The second step of this modular approach involves the azide–alkyne cycloaddition click reaction. The versatility of the two-step approach has been exemplified by the selective incorporation of fluorescent dyes and a positron-emitting copper-64 radiotracer for fluorescence and positron-emission tomography imaging of activated platelets, platelet aggregates, and thrombi, respectively. This flexible and versatile approach could be readily adapted to incorporate a large array of tailor-made functional groups using reliable click chemistry whilst preserving the activity of the antibody or other sensitive biological macromolecules.*

The attachment of small molecules, nanoparticles, and imaging agents to recombinant proteins such as antibodies offers exciting possibilities in the quest for better diagnostics and therapeutics.[1] Conventional strategies include reacting electrophilic groups such as isothiocyanates and carboxylic acids with the amine group of lysine,[2] or Michael addition with the thiol present in cysteine.[3] Under certain conditions, reactions involving sulfhydryl groups are reversible in vivo[4] and non-specific conjugation to lysine can compromise protein function.[2,5] In contrast, site-specific conjugation provides homogeneity and improved outcomes in the retention of biological function.[6] Orthogonal groups for site-specific conjugation can be introduced into proteins by genetic modification using amber codons and feeding the host organism amino acids with orthogonal groups.[7,8] This approach requires special plasmids, expression systems, and expensive cell media supplements, and in some cases overall yields are low.[9] Enzymatic protein modification is emerging as an attractive alternative as it can generate high yields while proceeding under mild conditions. Among other approaches,[10,11] the Sortase A (SrtA) enzyme from *Staphylococcus aureus* has been extensively used for protein engineering[12,13] and antibody modification.[14–18] SrtA recognizes substrate proteins bearing a short recognition motif (LPXTG) and cleaves the peptide between threonine and glycine forming a new bond with nucleophiles containing N-terminal glycine residues.[19] In most cases the reaction does not interfere with function; however, to obtain high yields, a high molar excess of SrtA and the nucleophile over the LPXTG substrate is required, which is one of the main shortcomings of this approach. Herein we present the use of SrtA for the site-specific incorporation of orthogonal alkyne functional groups into single-chain antibodies (scFvs) to enable further modification by cycloaddition click reactions. The Cu^{I}-catalyzed azide–alkyne cycloaddition (CuAAC), a variant of the Huisgen azide–alkyne cycloaddition, produces 1,4-substituted triazoles from the reaction of azides and terminal alkynes with essentially perfect regioselectivity.[20,21] In instances where it is necessary to avoid the use of Cu^{I} as a catalyst, the strain-promoted azide–alkyne cycloaddition (SPAAC) reaction of azides with strained cyclooctynes is a bioorthogonal alternative (Figure 1).[22]

[*] Dr. K. Alt, S. Jagdale, K. Ardipradja, Dr. G. Y. Krippner, Prof. C. E. Hagemeyer[+]
Vascular Biotechnology, Baker IDI
Melbourne (Australia)
E-mail: karen.alt@bakeridi.edu.au
christoph.hagemeyer@bakeridi.edu.au

Dr. B. M. Paterson, S. E. Rudd, T. U. Connell, Prof. P. S. Donnelly
School of Chemistry/Bio21 Institute
University of Melbourne (Australia)
E-mail: pauld@unimelb.edu.au

Dr. E. Westein, A. K. N. Nair, Dr. X. Wang, Prof. K. Peter[+]
Atherothrombosis and Vascular Biology, Baker IDI
Melbourne (Australia)

S. S. Poniger, Prof. H. J. Tochon-Danguy
Department of Molecular Imaging and Therapy, Austin Health
Melbourne (Australia)

[+] These authors contributed equally to this work.

[**] This work was funded by the National Health and Medical Research Council (NHMRC), Grants 1029249, 1017670 and 1011418 as well as the Australian Research Council (P.S.D.). K.Al. is supported by the German Research Foundation (Al 1521/1-1). B.M.P. is supported by a Victorian Postdoctoral Research Fellowship funded by the Victorian Government. K.Ar. is supported by the NHMRC and the National Heart Foundation (586740). P.S.D. is an Australian Research Council Future Fellow. K.P. is a Principal Research Fellow of the NHMRC. C.E.H. is a National Heart Foundation Career Development Fellow. This research was undertaken using equipment provided by Monash Biomedical Imaging, Monash University as part of the Victorian Biomedical Imaging Capability (Victorian Government). The work was also supported in part by the Victorian Government's Operational Infrastructure Support Program, Victoria's Science Agenda Strategic Project Fund, and the PET Solid Target Laboratory, an ANSTO-Austin-LICR Cyclotron Partnership.

Supporting information for this article is available on the WWW under http://dx.doi.org/10.1002/anie.201411507.

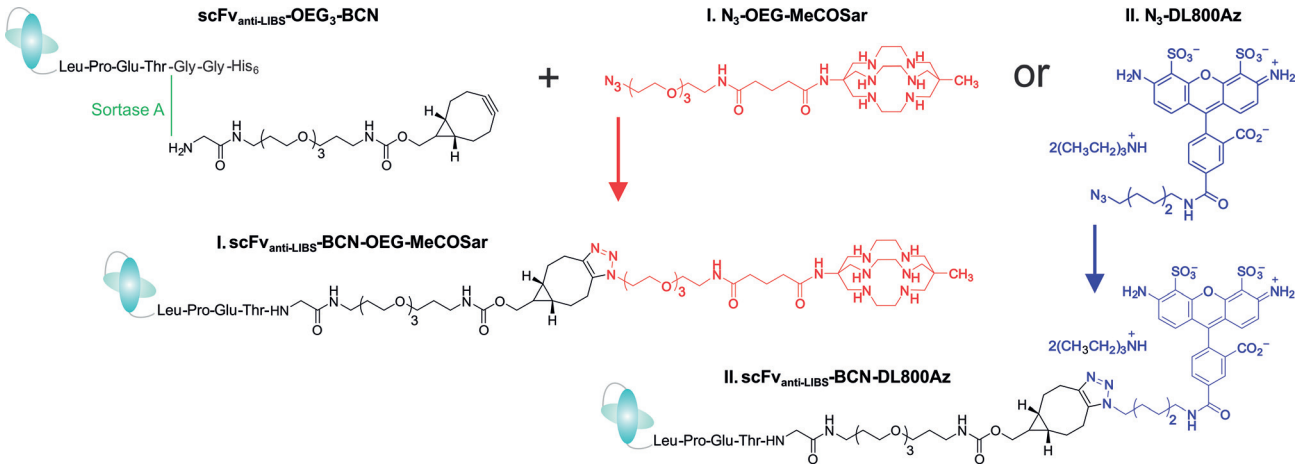

Figure 1. Overview of the two-step bio-click site-specific modification of scFv$_{anti-LIBS}$-LPETGG-His$_6$ with Gly-OEG$_3$-BCN followed by the fluorescent dye DL800Az or the macrobicyclic cage amine sarcophagine ligand N$_3$-OEG-MeCOSar.

We have employed two short bifunctional linkers consisting of a single N-terminal glycine residue linked through an oligoethylene glycol (OEG) to either a terminal alkyne (Gly-OEG$_4$-alkyne) or to bicyclo-[6.1.0]-nonyne (BCN), a cyclooctyne that benefits from a high rate of reaction and a single regioisomeric triazole product (Gly-OEG$_3$-BCN) (Supporting Information, Figure S1). The short linkers and SrtA required are readily available in larger quantities from chemical synthesis and *E.coli* production respectively, making our system suitable for scale-up productions. The SrtA was used to catalyze the modification of a scFv$_{anti-LIBS}$[23,24] that binds selectively to activated platelets by targeting ligand-induced binding sites (LIBS) on the glycoprotein IIb/IIIa (αIIbβ3, CD41/CD61) receptor.[25,26] This integrin receptor undergoes a conformational change upon platelet activation, exposing epitopes that are uniquely specific for activated platelets.[27] Selectivity for activated platelets is of interest as they play important roles in atherosclerosis, thrombosis, and inflammation.[28,29]

ScFv$_{anti-LIBS}$-LPETGG and SrtA were produced with a His$_6$ affinity tag at the C-terminus. The bifunctional linkers Gly-OEG$_4$-alkyne and Gly-OEG$_3$-BCN were allowed to react with scFv$_{anti-LIBS}$-LPETGG in the presence of SrtA for 5 h at 37 °C and the products were purified by affinity chromatography. The reaction yields obtained using Gly-OEG$_4$-alkyne and Gly-OEG$_3$-BCN were 87 % and 89 %, respectively. The deconvoluted ESI mass spectra of scFv$_{anti-LIBS}$-BCN and scFv$_{anti-LIBS}$-alkyne are shown in Figure 2 A with the mass differences from scFv$_{anti-LIBS}$-LPETGG indicated. The mass differences correspond to the loss of the peptide cleaved during the SrtA reaction (3578 g mol^{-1}) plus the respective molecular weights of Gly-OEG$_3$-BCN (453 g mol^{-1}) and Gly-OEG$_4$-alkyne (288 g mol^{-1}).

The ability of the immunoconjugates to bind selectively to activated platelets was assessed using fluorescence-activated cell sorting (FACS) and indicated strong binding to the target receptor (Figure 2 B) even after modification. As reported before, the conjugates did not bind to non-activated platelets (Supporting Information, Figure S2 A/B). In addition,

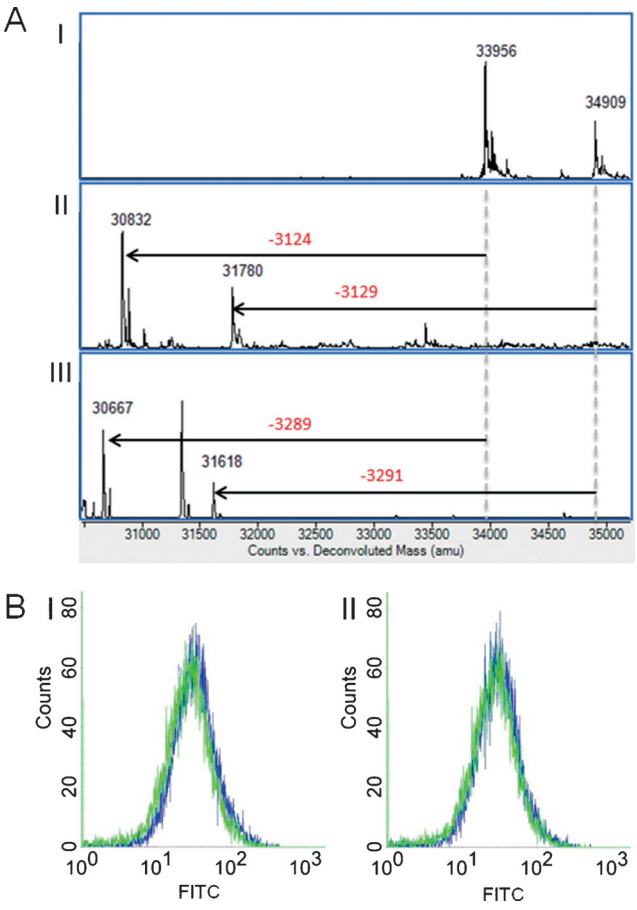

Figure 2. A) ESI mass spectrum of scFv$_{anti-LIBS}$ (I), scFv$_{anti-LIBS}$-BCN (II) and scFv$_{anti-LIBS}$-alkyne (III). The scFv is detected as two species with and without the leader signal only partially removed when translocating to the cell supernatant during protein production. The unlabeled peak in (III) is hydrolyzed scFv with no peptide attached. B) Histogram showing binding of non-modified scFv$_{anti-LIBS}$ (green line) to ADP-stimulated platelets compared to modified scFv$_{anti-LIBS}$-BCN (I)/scFv$_{anti-LIBS}$-alkyne (II) (blue line) in flow cytometry. Results indicate preserved binding of the scFv$_{anti-LIBS}$ constructs after Sortase and click modification. Representative histograms out of $n = 3$ are shown.

a mutant variant ($scFv_{mut}$) generated as control did not bind to activated platelets (Supporting Information, Figure S2 C/D). The versatility of the site-specifically alkyne- or BCN-modified scFvs was demonstrated with three azide-containing molecules: A near-infrared (NIR) emitting dye DyLight 800 (DL800Az), N_3-AlexaFluor-488, and a macrobicyclic cage amine sarcophagine ligand ideally suited to coordinate positron-emitting radioisotopes of copper for positron emission tomography (PET) (see the overview in the Supporting Information, Figure S3).

DL800Az was reacted with $scFv_{anti\text{-}LIBS}$-alkyne catalyzed by CuAAC to give $scFv_{anti\text{-}LIBS}$-alkyne-DL800 and $scFv_{anti\text{-}LIBS}$-BCN using SPAAC to give $scFv_{anti\text{-}LIBS}$-BCN-DL800. The reaction products were resolved on SDS-PAGE (Figure 3 A/B, showing Coomassie-stained scFv in the red channel;

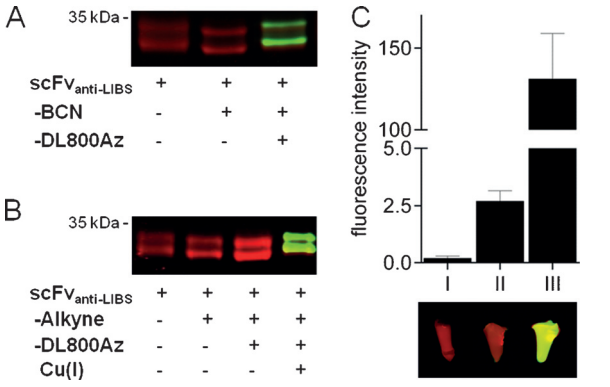

Figure 3. NIR imaging (excitation 685/785 nm, emission 700/800 nm) of coomassie brilliant blue stained SDS-PAGE gels demonstrate the generation of click chemistry modified $scFv_{anti\text{-}LIBS}$ using Srt A. A) $ScFv_{anti\text{-}LIBS}$ (35/34 kDa, with/without leader signal) compared to $scFv_{anti\text{-}LIBS}$-BCN (31.8/30.8 kDa) and SPAAC reacted $scFv_{anti\text{-}LIBS}$-BCN-DL800Az. B) $ScFv_{anti\text{-}LIBS}$ compared to $scFv_{anti\text{-}LIBS}$-alkyne (31.6/30.7 kDa) and CuAAC reacted $scFv_{anti\text{-}LIBS}$-alkyne-DL800Az without/with Cu^{I} catalyst. C) Specific binding of $scFv_{anti\text{-}LIBS}$-BCN-DL800Az to in vitro formed human thrombi ($n=3$). Relative fluorescence intensities (top) and representative images (bottom) of I) PBS control, II) $scFv_{mut}$-BCN-DL800Az control antibody, and III) $scFv_{anti\text{-}LIBS}$-BCN-DL800Az.

complete gels in the Supporting Information, Figure S4). The click-modified scFv with the dye attached is detected at a higher molecular weight and no non-modified scFv is visible, indicating full completion of the reaction.

To evaluate the targeting ability of the functionalized scFv, binding to activated GPIIb/IIIa on thrombi was examined by NIR imaging. Thrombi were formed from human platelet rich plasma and incubated with $scFv_{anti\text{-}LIBS}$-BCN-DL800 and $scFv_{mut}$-BCN-DL800. $ScFv_{anti\text{-}LIBS}$-BCN-DL800 demonstrated high specific binding compared with $scFv_{mut}$-BCN-DL800, thus indicating the preserved targeting ability of $scFv_{anti\text{-}LIBS}$ after two-step modification (Figure 3 C).

Selective binding of the modified $scFv_{anti\text{-}LIBS}$-BCN was also examined by immunofluorescence microscopy. The alkyne group of $scFv_{anti\text{-}LIBS}$-BCN was conjugated to the azide-functionalized dye N_3-AlexaFluor-488 (AF488) using SPAAC click chemistry followed by incubation for 1 h in the dark with platelets adhered to a collagen matrix. The

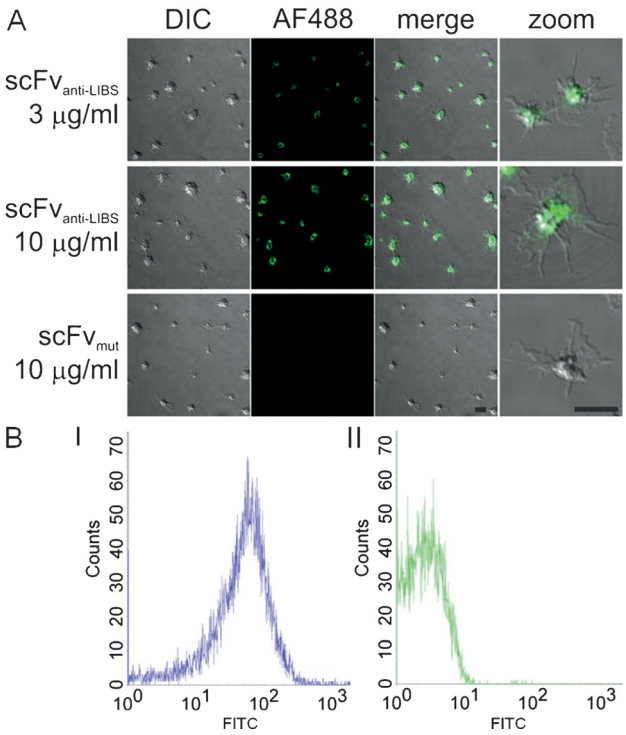

Figure 4. Immunofluorescence microscopy experiments showing specific binding to activated platelets. A) DIC, AF488 (fluorescence), merge and zoom images showing that the modified antibody $scFv_{anti\text{-}LIBS}$-BCN-AF488 binds in a concentration-depended manner to collagen adherent activated platelets whereas the control $scFv_{mut}$-BCN-AF488 does not bind (scale bar 5 µm). B) Flow cytometry histograms illustrating specific binding of (I) $scFv_{anti\text{-}LIBS}$-BCN-AF488 to activated platelets compared to (II) non-binding $scFv_{mut}$-BCN-AF488 (both 3 $\mu g\,mL^{-1}$).

fluorescence signal showed a strong concentration dependent binding to activated platelets compared to the mutated version, again confirming preserved functionality (Figure 4 A). Activation specific binding of this construct was also confirmed in flow cytometry (Figure 4 B).

Bifunctional chelators based on the macrobicyclic cage amine sarcophagine ligands are well-suited for ^{64}Cu radioimmunoconjugates because of the rapid room-temperature chelation kinetics and high in vivo stability. Click chemistry has been increasingly applied to bioconjugation in the development of new molecular imaging probes.[30,31] Previously, a diazido sarcophagine chelator was conjugated to an NGR-containing peptide using SPAAC chemistry, radiolabeled with ^{64}Cu, and investigated for microPET imaging of CD13 receptor expression in mice.[32] To demonstrate the two-step sortase click chemistry approach, the bifunctional chelator MeCOSar[33] was elaborated with a short-chain OEG linker with an azide functional group to give N_3-OEG-MeCOSar (Supporting Information, Figure S5).

To avoid adversely affecting specific activity owing to coordination of Cu^{II} by the sarcophagine chelator during the CuAAC reaction, N_3-OEG-MeCOSar was pre-incubated with $^{64}Cu^{II}$ before conjugation to $scFv_{anti\text{-}LIBS}$-alkyne. N_3-OEG-MeCOSar was conjugated to $scFv_{anti\text{-}LIBS}$-BCN using SPAAC chemistry and the resulting conjugate was radiolabeled with $^{64}Cu^{II}$ at pH 7 and room temperature in <30 min.

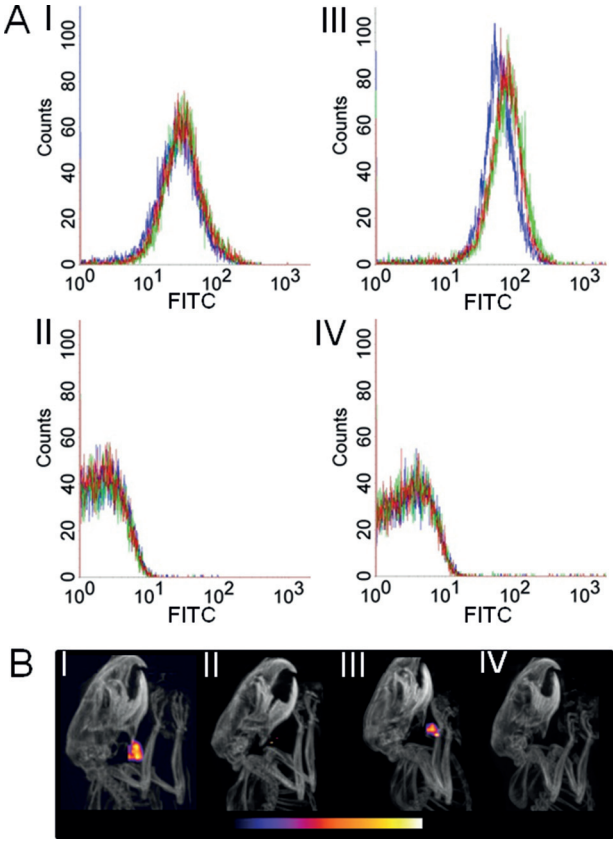

Figure 5. A) FACS analysis of modified antibodies to activated and non-activated human platelets. Histogram shows binding of non-modified $scFv_{anti\text{-}LIBS}$-BCN (I)/$scFv_{anti\text{-}LIBS}$- alkyne (III) (blue line) to ADP-stimulated platelets compared to modified $scFv_{anti\text{-}LIBS}$-BCN-OEG-MeCOSar/$scFv_{anti\text{-}LIBS}$-alkyne-OEG-MeCOSar (green line) and radiolabelled $scFv_{anti\text{-}LIBS}$-BCN-OEG-^{64}CuMeCOSar/$scFv_{anti\text{-}LIBS}$-alkyne-OEG-^{64}CuMeCOSar (red line) in flow cytometry. Results indicate preserved binding of the $scFv_{anti\text{-}LIBS}$ constructs after modification, click reaction and ^{64}Cu loading. $ScFv_{mut}$ constructs (BCN II/alkyne IV) showed no binding to activated platelets. Representative histograms out of $n=3$ are shown. B) Serial small-animal PET imaging in the model of mouse carotid artery thrombosis 60 min after injection of the radiotracer. Comparison of representative maximum-intensity projection PET images of $scFv_{anti\text{-}LIBS}$-BCN-OEG-^{64}CuMeCOSar (I)/$scFv_{anti\text{-}LIBS}$-alkyne-OEG-^{64}CuMeCOSar (III) and $scFv_{mut}$-BCN-OEG-^{64}CuMeCOSar (II)/$scFv_{mut}$-alkyne-OEG-^{64}CuMeCOSar (IV). The color scale for all PET image data shows radiotracer uptake with white corresponding to the highest activity and blue to the lowest activity.

The antigen binding of the $^{64}Cu^{II}$ radiolabeled conjugates were comparable to that of copper-free $scFv_{anti\text{-}LIBS}$-LPET-BCN/alkyne and the unmodified $scFv_{anti\text{-}LIBS}$, and none of these constructs bound to non-activated platelets (Figure 5; Supporting Information, Figure S6).

The targeting abilities of the ^{64}Cu radiolabeled immunoconjugates $scFv_{anti\text{-}LIBS}$-BCN/alkyne-OEG-^{64}CuMeCOSar and $scFv_{mut}$-BCN/alkyne-OEG-^{64}CuMeCOSar toward activated platelets were evaluated in an in vivo model of mouse carotid artery thrombosis induced by exposure to $FeCl_3$.

The biodistribution data confirmed a significant increase in $scFv_{anti\text{-}LIBS}$-BCN/alkyne-OEG-^{64}CuMeCOSar uptake in the injured vessel compared to the non-injured vessel and muscle (Table 1). There was also significantly higher uptake

Table 1: Biodistribution of the radiolabeled immunoconjugates $scFv_{anti\text{-}LIBS}$-BCN/alkyne-OEG-^{64}CuMeCOSar and $scFv_{mut}$-BCN/alkyne-OEG-^{64}CuMeCOSar in an in vivo model of mouse carotid artery thrombosis at 90 min after tracer injection.

scFv-BCN-OEG-^{64}CuMeCOSar:

Tissue	Non-blocking ($n=4$)	$scFv_{anti\text{-}LIBS}$-Blocking ($n=3$)	$scFv_{mut}$-Non-blocking ($n=3$)
Injured V	17.63 ± 2.97	3.68**** ± 0.93	4.71*** ± 1.51
Control V	2.03**** ± 1.33	2.32 ± 1.65	1.81 ± 0.49
Muscle	0.72**** ± 0.53	0.29 ± 0.19	0.17 ± 0.17

scFv-alkyne-OEG-^{64}CuMeCOSar:

Tissue	$scFv_{anti\text{-}LIBS}$-Non-blocking ($n=5$)	$scFv_{mut}$-Non-blocking ($n=5$)
Injured V	15.45 ± 9.42	6.9* ± 2.72
Control V	5.23* ± 2.70	5.85 ± 2.38
Muscle	0.43** ± 0.53	0.55 ± 0.33

(Data are %ID/g, expressed as mean ± SD; *$P<0.05$, **$P<0.01$, ***$P<0.001$ and ****$P<0.0001$; compared to injured V (vessel)).

of $scFv_{anti\text{-}LIBS}$-BCN/alkyne-OEG-^{64}CuMeCOSar in the injured vessel compared to $scFv_{mut}$-BCN/alkyne-OEG-^{64}CuMeCOSar. In a separate study, administration of $scFv_{anti\text{-}LIBS}$ (400 μg) 30 min before radiotracer injection to block the binding sites significantly reduced $scFv_{anti\text{-}LIBS}$-BCN-OEG-^{64}CuMeCOSar binding to the target receptor (Table 1). Furthermore, the mice were placed in a small-animal PET/CT 30 min post-injection of a single dose of $scFv_{anti\text{-}LIBS}$-BCN/alkyne-OEG-^{64}CuMeCOSar or $scFv_{mut}$-BCN/alkyne-OEG-^{64}CuMeCOSar (3–5 MBq) with the carotid artery set as the region of interest. The PET/CT scans showed an accumulation of $scFv_{anti\text{-}LIBS}$-BCN/alkyne-OEG-^{64}CuMeCOSar in the injured vessel and no significant uptake of $scFv_{mut}$-BCN/alkyne-OEG-^{64}CuMeCOSar confirming the highly specific GPIIb/IIIa mediated binding (Figure 5B).

Both methods, CuAAC and SPAAC, resulted in homogeneous products performing identically in the in vitro and in vivo tests. The absence of co-factors such as Cu and ascorbate as well as the ability to pre-form the conjugate outweighs the slower reaction kinetics of the SPAAC compared to CuAAC, making SPAAC the preferred assembly route.

In summary, we have developed a convenient and simple two-step modular system consisting of enzyme-mediated bioconjugation followed by click chemistry and demonstrated the site-specific and reproducible modification of a scFv. We demonstrated that this functionalization technique can be used for various applications including fluorescence cellular studies to in vivo molecular imaging using biological macromolecules. Our approach is not limited to the scFv format and can be used with all biomolecules as long as the C-terminus is not essential for function and accessible for the Sortase enzyme. Site-specific conjugation can improve the stability, activity, and homogeneity of protein and antibody therapeutics and expand the utility of antibodies into many exciting future applications, ensuring a highly promising position for these powerful molecules at the forefront of diagnostic imaging and therapeutics.

Keywords: bioconjugation · click chemistry · fluorescence imaging · PET imaging · Sortase A

How to cite: *Angew. Chem. Int. Ed.* **2015**, *54*, 7515–7519
Angew. Chem. **2015**, *127*, 7625–7629

[1] B. Y. S. Kim, J. T. Rutka, W. C. W. Chan, *N. Engl. J. Med.* **2010**, *363*, 2434.
[2] K. Ardipradja, S. D. Yeoh, K. Alt, G. O'Keefe, A. Rigopoulos, D. W. Howells, A. M. Scott, K. Peter, U. Ackerman, C. E. Hagemeyer, *Nucl. Med. Biol.* **2014**, *41*, 229.
[3] J. R. Junutula, K. M. Flagella, R. A. Graham, K. L. Parsons, E. Ha, H. Raab, S. Bhakta, T. Nguyen, D. L. Dugger, G. Li, et al., *Clin. Cancer. Res.* **2010**, *16*, 4769.
[4] B.-Q. Shen, K. Xu, L. Liu, H. Raab, S. Bhakta, M. Kenrick, K. L. Parsons-Reponte, J. Tien, S.-F. Yu, E. Mai, et al., *Nat. Biotechnol.* **2012**, *30*, 184.
[5] K. Alt, B. M. Paterson, K. Ardipradja, C. Schieber, G. Buncic, B. Lim, S. S. Poniger, B. Jakoby, X. Wang, G. J. O'Keefe, et al., *Mol. Pharm.* **2014**, *11*, 2855.
[6] J. R. Junutula, H. Raab, S. Clark, S. Bhakta, D. D. Leipold, S. Weir, Y. Chen, M. Simpson, S. P. Tsai, M. S. Dennis, et al., *Nat. Biotechnol.* **2008**, *26*, 925.
[7] Z. Yu, Y. Pan, Z. Wang, J. Wang, Q. Lin, *Angew. Chem. Int. Ed.* **2012**, *51*, 10600; *Angew. Chem.* **2012**, *124*, 10752.
[8] A. J. De Graaf, M. Kooijman, W. E. Hennink, E. Mastrobattista, *Bioconjugate Chem.* **2009**, *20*, 1281.
[9] T. S. Young, P. G. Schultz, *J. Biol. Chem.* **2010**, *285*, 11039.
[10] P. M. Drake, A. E. Albers, J. Baker, S. Banas, R. M. Barfield, A. S. Bhat, G. W. de Hart, A. W. Garofalo, P. Holder, L. C. Jones, et al., *Bioconjugate Chem.* **2014**, *25*, 1331.
[11] C.-W. Lin, A. Y. Ting, *J. Am. Chem. Soc.* **2006**, *128*, 4542.
[12] M. W. Popp, J. M. Antos, G. M. Grotenbreg, E. Spooner, H. L. Ploegh, *Nat. Chem. Biol.* **2007**, *3*, 707.
[13] M. W.-L. Popp, H. L. Ploegh, *Angew. Chem. Int. Ed.* **2011**, *50*, 5024; *Angew. Chem.* **2011**, *123*, 5128.
[14] B. M. Paterson, K. Alt, C. M. Jeffery, R. I. Price, S. Jagdale, S. Rigby, C. C. Williams, K. Peter, C. E. Hagemeyer, P. S. Donnelly, *Angew. Chem. Int. Ed.* **2014**, *53*, 6115; *Angew. Chem.* **2014**, *126*, 6229.
[15] M. P. Madej, G. Coia, C. C. Williams, J. M. Caine, L. A. Pearce, R. Attwood, N. A. Bartone, O. Dolezal, R. M. Nisbet, S. D. Nuttall, et al., *Biotechnol. Bioeng.* **2012**, *109*, 1461.
[16] H. T. Ta, S. Prabhu, E. Leitner, F. Jia, D. von Elverfeldt, K. E. Jackson, T. Heidt, A. K. N. Nair, H. Pearce, C. von zur Muhlen, et al., *Circ. Res.* **2011**, *109*, 365.
[17] S. Möhlmann, C. Mahlert, S. Greven, P. Scholz, A. Harrenga, *ChemBioChem* **2011**, *12*, 1774.
[18] L. K. Swee, C. P. Guimaraes, S. Sehrawat, E. Spooner, M. I. Barrasa, H. L. Ploegh, *Proc. Natl. Acad. Sci. USA* **2013**, *110*, 1428.
[19] S. K. Mazmanian, G. Liu, H. Ton-That, O. Schneewind, *Science* **1999**, *285*, 760.
[20] V. V. Rostovtsev, L. G. Green, V. V. Fokin, K. B. Sharpless, *Angew. Chem. Int. Ed.* **2002**, *41*, 2596; *Angew. Chem.* **2002**, *114*, 2708.
[21] C. W. Tornøe, C. Christensen, M. Meldal, *J. Org. Chem.* **2002**, *67*, 3057.
[22] G. deAlmeida, E. M. Sletten, H. Nakamura, K. K. Palaniappan, C. R. Bertozzi, *Angew. Chem. Int. Ed.* **2012**, *51*, 2443; *Angew. Chem.* **2012**, *124*, 2493.
[23] C. E. Hagemeyer, C. von zur Muhlen, D. von Elverfeldt, K. Peter, *Thromb. Haemostasis* **2009**, *101*, 1012.
[24] C. E. Hagemeyer, M. Schwarz, K. Peter, *Semin. Thromb. Hemostasis* **2007**, *33*, 185.
[25] P. Stoll, N. Bassler, C. E. Hagemeyer, S. U. Eisenhardt, Y. C. Chen, R. Schmidt, M. Schwarz, I. Ahrens, Y. Katagiri, B. Pannen, et al., *Arterioscler. Thromb. Vasc. Biol.* **2007**, *27*, 1206.
[26] C. E. Hagemeyer, K. Peter, *Curr. Pharm. Des.* **2010**, *16*, 4119.
[27] P. C. Armstrong, K. Peter, *Thromb. Haemostasis* **2012**, *107*, 808.
[28] M. Gawaz, H. Langer, A. E. May, *J. Clin. Invest.* **2005**, *115*, 3378.
[29] A. E. May, P. Seizer, M. Gawaz, *Arterioscler. Thromb. Vasc. Biol.* **2008**, *28*, s5.
[30] K. Nwe, M. W. Brechbiel, *Cancer Biother. Radiopharm.* **2009**, *24*, 289.
[31] D. Zeng, B. M. Zeglis, J. S. Lewis, C. J. Anderson, *J. Nucl. Med.* **2013**, *54*, 829.
[32] G. Li, X. Wang, S. Zong, J. Wang, P. S. Conti, K. Chen, *Mol. Pharm.* **2014**, *11*, 3938.
[33] B. M. Paterson, P. Roselt, D. Denoyer, C. Cullinane, D. Binns, W. Noonan, C. M. Jeffery, R. I. Price, J. M. White, R. J. Hicks, et al., *Dalton Trans.* **2014**, *43*, 1386.

Received: November 28, 2014
Revised: February 24, 2015
Published online: May 11, 2015

